

Enhanced zeolite-polysulfone membranes for regenerable and antifouling dye removal

Yasmina Afir^{1a}, Nabila Cherifi^{2,3}, Adel Ouradi^{1,4} and Fatima Boukraa^{*5}

¹Laboratoire de Synthèse Macromoléculaire et Thioorganique Macromoléculaire, Faculté de Chimie, Université des Sciences et de la Technologie Houari Boumediene, USTHB, B.P 32 El-Alia, Algiers, Algeria

²Centre de Recherche Scientifique et Technique en Analyses Physico-chimiques (CRAPC), Zone Industrielle, BP 384 Bou-Ismaïl, Tipaza, Algeria

³Unité de Recherche en Analyses Physico-Chimiques des Milieux Fluides et Sols –(URAPC-MFS/ CRAPC), 11 Chemin Doudou Mokhtar, Ben Aknoun – Alger, Algeria

⁴Laboratoire Chimie Physique Moléculaire et Macromoléculaire, Université Saad Dahlab Blida 1, Route de Soumaa, BP 270, Blida, 09000, Algeria

⁵Faculté de Chimie, Université des Sciences et de la Technologie Houari Boumediene, USTHB, B.P 32 El-Alia, Algiers, Algeria

(Received September 29, 2024, Revised February 13, 2025, Accepted February 21, 2025)

Abstract. The growing environmental contamination from industrial dyes calls for more efficient and sustainable wastewater treatment technologies. This study presents a sustainable approach by developing polysulfone-based hybrid membranes, modified with natural zeolite which is a low-cost, eco-friendly material, at varying concentrations (0.5, 1, 2, and 3 wt%) using the phase inversion process. The use of zeolite as both a porogen and a hydrophilic agent is a key innovation that significantly enhances membrane performance. The membranes were characterized using SEM, TGA, and contact angle measurements, and their pure water permeability was tested. The membrane with 3 wt% zeolite achieved an outstanding pure water flux (PWF) of 151.5 L m⁻² h⁻¹ at 4 bar, marking a 30-fold improvement over unmodified polysulfone membranes. Performance tests with methylene blue (MB) and orange G dyes revealed that the optimized membrane (PSf/Z 3%) exhibited a flux recovery ratio (FRR%) of 86.31% and a 99.6% rejection rate for MB. This study not only demonstrates a substantial advancement in filtration performance but also highlights the environmental and cost benefits of using natural zeolite. By offering a scalable, efficient, and sustainable solution for dye removal, this research provides a practical approach to mitigating industrial pollution and reducing treatment costs.

Keywords: antifouling; nano-particles; polysulfone membrane; separation; water treatment

1. Introduction

Dyes play an important role in many aspects of our lives today. They are used to add aesthetic colour to a wide range of materials in industries as diverse as textiles, cosmetics, paper and petrochemicals. However, their production and extensive use can have adverse environmental effects, particularly in terms of water pollution (Imam *et al.* 2021). The wastewater generated accounts for 17–20 % of global water pollution (Routoula *et al.* 2020, He *et al.* 2023). These dyes are known to be highly stable in sunlight and resistant to biodegradation (Vakili *et al.* 2023), leading to long-term water pollution, and pose significant risks to aquatic ecosystems and human health due to their potential toxicity and carcinogenicity (Abdelhamid *et al.* 2020).

One of the dyes commonly used in industrial applications is methylene blue (MB), a cationic dye known for its high solubility in water and extensive use in the textile and food industries. Above a certain level, the consumption of MB causes adverse effects on human health such as high blood

pressure, abdominal pain, mental disorders and may even be carcinogenic (Cheikh S’Id *et al.* 2021, Rana *et al.* 2022). Several studies have focused on the removal of MB from water (Badrinezhad *et al.* 2018, Cheikh S’Id *et al.* 2021, Vedula and Yadav 2022).

Another dye of note is Orange G (OG), which is characterized as a mono-azo and anionic dye that remains water soluble and stable under a range of pH conditions. OG dye has been shown to have hazardous and unavoidable adverse effects on aquatic species and the aquatic environment as a whole. It has been reported as one of the most toxic anionic dyes, exhibiting chromosomal damage and clastogenic activity. Not only OG, but also the intermediates formed during its degradation are also toxic (Imam *et al.* 2021). Much research has focused on the elimination of these dyes (Salam *et al.* 2017, Banerjee *et al.* 2019, Laksaci *et al.* 2019). Therefore, it is of utmost importance to develop practical, cost-effective, and environmentally friendly technologies to effectively remove these pollutants from wastewater (Vakili *et al.* 2023). In recent years, a number of methods have been developed to remove dyes from wastewater. The problem of dye contamination can be mitigated by a number of biological, physical and chemical processes. Membrane rejection and batch adsorption are both separation and purification

*Corresponding author, Ph.D., Professor,
E-mail: fboukraa@usthb.dz

^a Ph.D. Student, Email: yafir@usthb.dz

processes, but they differ in their mechanisms and applications. Membrane rejection relies on a physical barrier (the membrane) to separate components, operating on the basis of size, charge or solubility, and can be operated continuously. In contrast, batch adsorption depends on the affinity of the dissolved species for a solid surface and involves specific interactions between the adsorbate and the adsorbent, and typically operates in a batch mode where the adsorbent is mixed with the liquid phase for a period of time prior to separation. In addition, membrane systems are relatively easy to clean and regenerate, whereas the regeneration of adsorbents in batch adsorption often requires additional steps such as desorption. Previous research has shown that, in this context, membrane separation is an effective and environmentally friendly technology for the treatment of wastewater contaminated with dyes (Lekena *et al.* 2023).

Polymeric membranes are gaining increasing acceptance in water treatment due to their porous structure, strong mechanical properties, cost effective processes and operational requirements. However, these materials often have limitations in terms of separation performance that need to be improved. Developing membranes with superior performance and thermal stability remains a real challenge (Badrinezhad *et al.* 2018). Nanomaterials play an important role in solving problems related to water purification concerns and quality improvement. Recently, a number of porous inorganic fillers, such as zeolites, known for their exceptional separation capabilities, have been used to modify polymeric membranes.

Zeolites play a crucial role in enhancing membrane performance due to their high surface area, tunable pore structure, and selective adsorption properties. Environmentally, zeolites are beneficial as they are naturally abundant, non-toxic, and help in reducing the environmental impact of industrial pollutants by effectively removing contaminants like heavy metals and dyes from wastewater. Additionally, zeolites offer a cost-effective solution compared to other advanced materials, making them a sustainable choice for large-scale industrial applications (Abd Hamid *et al.* 2021, Ali *et al.* 2021, Shi *et al.* 2022). In addition, hybrid membrane separation technology offers a promising technical route by enabling both the removal and recovery of synthetic dyes from wastewater (Moradihamedani 2022). Hydrophilic elements have been incorporated to significantly improve the dye removal efficiency of the membrane (Abdelhamid *et al.* 2020, Benkhaya, Lgaz *et al.* 2021, Cheikh S'Id *et al.* 2021).

Polysulfone (PSf) is a hydrophobic polymer commonly used in the manufacture of membranes and is known for its excellent film forming properties and high mechanical and chemical stability. PSf based membranes have been the subject of numerous studies for their application in water treatment (Alawady *et al.* 2020, Asif *et al.* 2021, Benkhaya *et al.* 2023). Although polysulfone membrane separation processes exhibit outstanding advantages, they suffer from some limitations. The most important one is membrane fouling and consequent blockage of the membrane pores because of their hydrophobic nature (Sharma *et al.* 2017), leading to a drop in flux, separation efficiency, and consequently increasing costs (Mokhtari *et al.* 2017). While many studies have made significant progress in mitigating

these limitations, further improvements are still required. This study contributes to enhancing these properties and extending membrane lifetime, particularly by addressing fouling issues.

In this work, PSf was used as a polymer matrix to prepare ultrafiltration membranes by the phase inversion process. In order to improve membrane properties, zeolite-Y was added to the membrane doping solution at different weight ratios (0.5, 1, 2 and 3 wt. %). The mixed matrix PSf/zeolite nanocomposite membranes and the pure PSf membrane were characterized by various analytical techniques, to obtain an in-depth understanding of their chemical composition and structural morphology, and then their permeability to pure water was tested to evaluate their performance.

Finally, as part of an application, the MB and OG removal performance of the different membranes prepared was determined and compared. To the best of our knowledge, no study has been carried out on the removal of the two dyes MB and OG from water using a PSf/zeolite hybrid membrane at different concentrations.

2. Materials and experiments

2.1 Materials

Analytical grade chemicals were used as received without any further processing. Polysulfone resin pellets (PSf, Udel P-3500, Mw: 35000 Da) used as membrane material were supplied by Solvay Advanced Polymer (Belgium). N-methyl-2-pyrrolidone (NMP, 99%) purchased from Fluka was used as the solvent. Zeolite Y powder was manufactured by ZEOLIST International, marketed under the name (CBV760, with a unit cell size of 24.24 Å) as indicated. The same as that used by (Ghribi *et al.* 2022). This zeolite powder exhibited a particle size distribution between 300 and 900 nm and was used both as an additive and an adsorbent. Deionized water was used as a coagulation bath for membrane solidification. Methylene blue and orange G were provided by Sigma Aldrich.

2.2 Membrane preparation

Flat polysulfone-based membranes were prepared by the conventional phase inversion method. The membranes were prepared according to the amounts of polymer and additives listed in Table 1.

Polysulfone pellets were first dissolved in NMP under continuous stirring at room temperature. Various amounts of zeolite were then added to the polymer solutions while stirring at 300 rpm, until a dispersed solution was obtained (~24 h). The resulting homogeneous solutions were allowed to stand for 1 hour without stirring to eliminate air bubbles, then poured and cast uniformly onto a glass plate using a casting knife. The casting solution was then immediately immersed in a coagulation bath containing distilled water maintained at a controlled temperature (25°C). To remove residual NMP, the resulting membrane was washed three times with deionized water before use. A pure PSf membrane was prepared by dissolving 16 wt% PSf pellets

Table 1 Composition of the casting solutions

Membrane	PSf (wt%)	Zeolite (wt%)	NMP
PSf/Z 0%		0	84
PSf/Z 0.5%		0,5	83.5
PSf/Z 1%	16	1	83
PSf/Z 2%		2	82
PSf/Z 3%		3	81

in NMP, in order to compare its results with those of mixed matrix membranes containing zeolite.

2.3 Membrane characterization

2.3.1 Pure water flux

The pure water flux (PWF) is a crucial factor for all types of membranes, as it is directly related to the number and size of the membrane pores. PWF was measured using a dead-end filtration cell (model 8050, 50 ml, Amicon, effective surface area = 13.4 cm²) connected to a nitrogen pressure source. Each membrane was soaked in deionized water for 24 hours prior to filtration, then pre-compacted with deionized water for 30 minutes at 1 bar. Pure water flux and hydraulic permeability were determined over a pressure range of 0.6, 1, 2, 3, and 4 bar using the following Eqs. (1)-(2) :

$$PWF = V / (A \times \Delta t) \quad (1)$$

$$Lp = PWF / \Delta P \quad (2)$$

where *PWF*: the pure water flux (L m⁻² h⁻¹), *V*: the filtrate volume (L), *A*: the membrane area (m²), *Δt*: the filtration time (h), *Lp*: the hydraulic permeability (L m⁻² h⁻¹ bar⁻¹) and *ΔP*: the trans-membrane pressure (TMP) (bar).

2.3.2 Contact angle analysis, porosity and pore size

To determine the hydrophobic and hydrophilic characteristics of the membranes, the contact angle was measured using the "GBX DIGIDROP" tensiometer. The volume of the drop of deionized water deposited on the surface of the membranes was 3 μl. An average of five measurements was taken on different parts of the surface of the dry membrane. The porosity of the membrane was determined by the dry-wet weight method. The membrane samples were cut into 3×3 cm squares and immersed in distilled water for 24 hours. After removing the excess water from the surface, the samples were weighed. The membrane samples were then dried in an oven at a temperature of 50 °C until a constant mass was obtained (~24 h). The dry membranes were then reweighed. Porosity was calculated from the measurements of both wet and dry sample weights. To minimize error, three pieces of each membrane were cut and tested.

The membrane porosity (*P* %) was obtained using Eq. (3):

$$P \% = (W_w - W_d / A \times L \times \rho) \times 100 \quad (3)$$

where *W_w* is the wet sample weight (g), *W_d* is the dry sample weight (g). *A*, *L* and *ρ* are the sample area (cm²), the sample thickness when wet (cm) and the pure water density (g/cm³), respectively.

The Guerout-Elford-Ferry (Eq. (4)) was used to calculate the mean pore radius (*r_m*):

$$r_m = \sqrt{(2.9 - 1.75 P) \times 8\eta l Q / P \times A \times \Delta P} \quad (4)$$

where, *r_m* is the mean pore radius, (m), *P* is the porosity (%), *η* is the viscosity of water (8.94 10⁻⁴ Pa.s), *l* is the membrane thickness (m), *Q* is the permeate volume of water per unit of time (m³/s), *A* : membrane area (m²), *ΔP* is the applied transmembrane pressure (105 Pa).

2.3.3 Scanning Electron Microscopy (SEM) analysis

The morphology of the prepared membranes was visualized by scanning electron microscopy (Philips XL30ESEM-FEG), both in cross-section and on the surface. For cross-sectional images, membrane samples were fractured in liquid nitrogen and then coated with a thin layer of gold.

2.3.4 Thermogravimetric Analysis (TGA)

To study the thermal stability, the prepared membranes were subjected to a thermal degradation test using a "Mettler Toledo TGA 2 Star" thermogravimeter. Alumina crucibles were used for the sample analysis. The analysis temperature was programmed between 25 and 700 °C at a heating rate of 20 °C/min, under a nitrogen atmosphere.

2.3.5 Dyes removal efficiency

The dye rejection efficiency of the membranes was evaluated for the pollutants MB and OG, using a filtration cell (Amicon 8050) placed under a magnetic stirrer. Aqueous solutions of MB and OG were prepared at a concentration of 10 ppm in freshly distilled water (pH between 6 and 7) and filtered separately through the membranes at a TMP of 2 bar and at room temperature. For each of membrane type and dye, three experiments were performed and the average was taken.

The concentrations of MB and OG in the feed and filtrate solutions were then measured using a "LAMBDA 20, Perkin Elmer" UV spectrophotometer. The maximum wavelengths were 665 and 448 nm for MB and OG, respectively. The dye rejection (R%) was determined using Eq. (5):

$$R\% = (1 - C_p / C_f) \times 100 \quad (5)$$

where *C_f* and *C_p* are the concentrations of the dyes substances in the feed and permeate streams, respectively. In addition, the methylene blue permeate flux (MBF) of the optimized PSf/Z 3% membrane was also evaluated over different pressures (0.6, 1, 2, 3, and 4 bar) to assess the stability the membrane during the ultrafiltration process.

2.3.6 Antifouling study

One of the main drawbacks of PSf membranes is the accumulation of deposits on their surface, some of which are irreversible and lead to pore blockage. The fouling

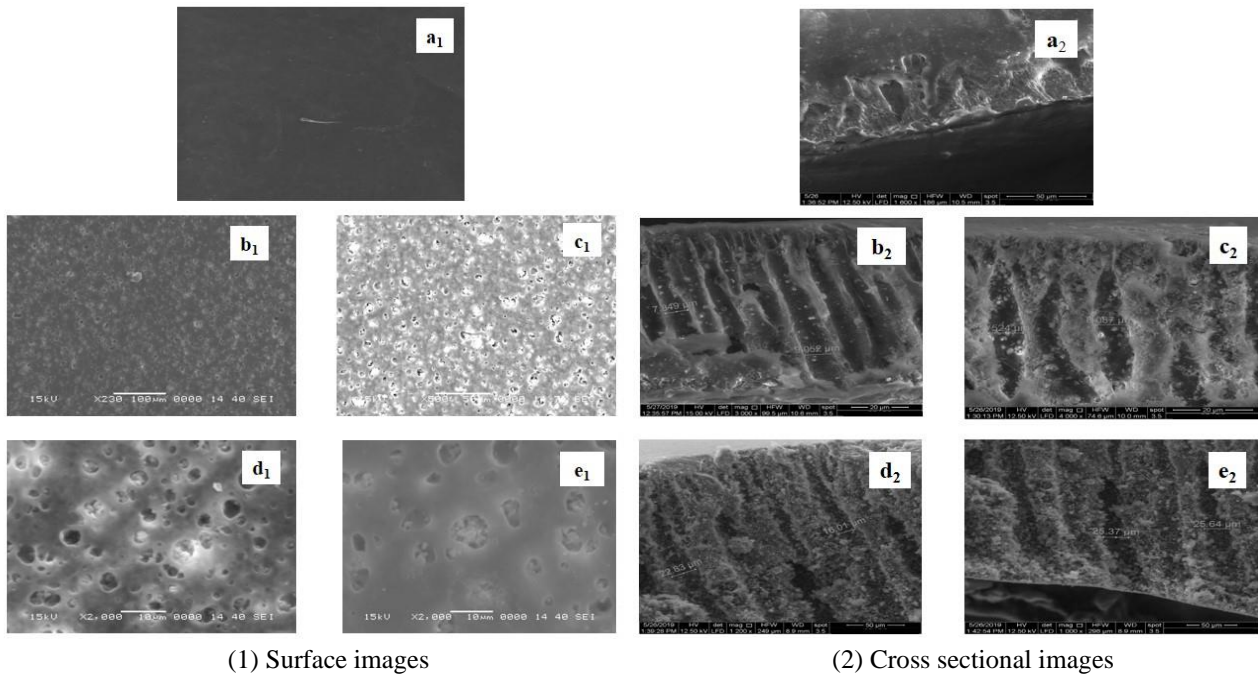


Fig. 1 SEM micrographs of the: a: 0 wt%, b: 0,5 wt%, c: 1 wt%, d: 2 wt% and e: 3 wt% PSf/Z membranes

behavior of the membranes was investigated using the existing literature (Ibrahim *et al.* 2016). To evaluate the antifouling performance of the synthesized membranes, the pure water flux (PWF 1) was tested at a transmembrane pressure (TMP) of 4 bar. An aqueous solution of 10 ppm MB was then introduced into the ultrafiltration system, and the MB dye was filtered for 1 hour. The flux for the MB solution, based on the amount of water permeating the membranes, was measured as (MBF). The membranes were then washed thoroughly with distilled water overnight. The pure water flux was measured again to obtain PWF 2, which was used to calculate the flux recovery ratio percentage (FRR%) as follows using Eq. (6):

$$\text{FRR \%} = \text{PWF 2} / \text{PWF 1} \quad (6)$$

2.3.7 The reusability of the membrane

The PSf/Z 3% composite membrane was selected for a regeneration study. The membrane was exposed to a 10 mg/L methylene blue (MB) solution for 1 hour at a constant transmembrane pressure (TMP) of 2 bar at room temperature. The used membrane was then reused to filter the same MB solution, and the resulting permeate was collected to measure the rejection rate. This experiment was repeated for up to 8 cycles (8 hours), maintaining the same initial concentration throughout the study, and the percentage rejection of MB dye was calculated for each cycle.

3. Results and discussion

3.1 SEM analysis

In order to observe the effect of the zeolite addition on

the morphology of the prepared membranes, the front view and cross-sectional SEM micrographs of pure PSf and PSf/zeolite hybrid membranes (0.5 to 3 wt%) are shown in Fig. 1. The presence of zeolite particles had a significant effect on the surface structure of the modified membranes. SEM images of the membrane surfaces (Fig. 1 (b₁)-(c₁)) show a uniform distribution of zeolite particles in the polymer matrix, resulting in a progressive increase in porosity over the entire surface of the different hybrid membranes compared to the smooth, non-porous surface of the pure PSf membrane (Fig. 1(a₁)). However, when the zeolite loading in the membrane exceeds 1 wt%, the uniform distribution ceases, and the zeolite nanoparticles become highly agglomerated (Fig. 1 (d₁)-(e₁)).

SEM micrographs of the cross-section of all the membranes show a typical asymmetric structure, with a dense upper layer (the side in contact with the coagulation bath) and a porous lower layer with finger-like pores and larger macrovoids at the bottom of the structure (the side in contact with the glass plate). This configuration causes instantaneous phase separation between the surface of the polymer solution and the water of the coagulation bath, resulting in the formation of a polymer-rich phase and a polymer-poor phase within the membrane structure (Hung *et al.* 2016, Nadour *et al.* 2017, Ouradi *et al.* 2020). The zeolite particle size distribution (300–900 nm) plays a crucial role in shaping the porous structure and overall performance. The tendency of larger particles to agglomerate due to van der Waals forces can lead to the formation of macrovoids and an increase in pore size, enhancing membrane permeability. Conversely, smaller particles can occupy the spaces between larger ones, promoting a more interconnected pore network (Adam *et al.* 2020, Zhu *et al.* 2024).

In particular, increasing the zeolite content (0 to 3 wt %)

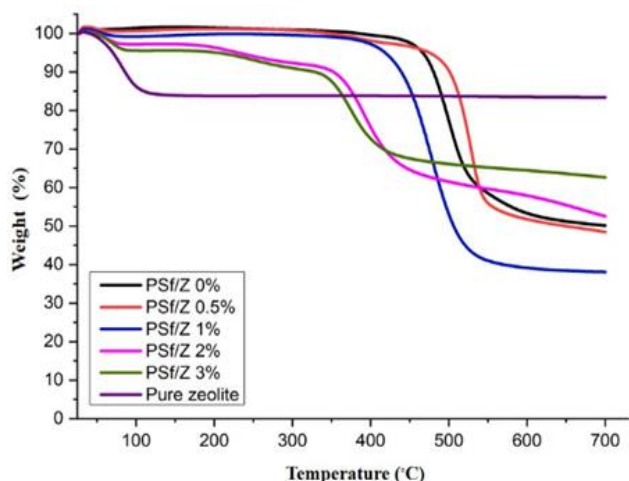


Fig. 2 TGA curves of pure Zeolite, neat PSf and PSf/Z membranes

in the casting solution, results in the formation of larger macrovoids and an increase in pore size (Liu *et al.* 2014) speculated that the higher zeolite content easily penetrated the coagulation bath due to its high affinity for water as a pore forming agent, resulting in the formation of additional surface pores and finger-like pores in the cross-section.

The interfacial incompatibility between the zeolite nanoparticles and the polymer, was verified by infrared analysis, as well as the brittleness and the aggregation of the particles. According to (Dorosti *et al.* 2011) the main factor contributing to this structural phenomenon can be attributed to the limited interactions between the polymers and the zeolite, coupled with the incongruence between the organic and inorganic properties of the polymer and the zeolite.

3.2 TGA analysis

The thermal stability of pure PSf, PSf/Z membranes and zeolite powder was investigated by TGA analysis between 25 °C and 700 °C, and the results are shown in Fig. 2.

The TGA curve of the pure PSf membrane (PSf/Z 0%) shows that polysulfone is a thermally stable polymer, that degrades at elevated temperatures with a single degradation step starting at 445.72°C, and continuing up to a temperature of 519.66°C, which means that the polymer decomposes with a weight loss of 65%. This resistance is attributed to the aromatic rings in the PSf chain, which together with the sulfone group incorporated in a conjugated system, provide a significant degree of stabilization.

The thermogram of pure zeolite shows that there is no degradation, which is likely to occur above 500°C. The mass loss observed around 100°C corresponds to the evaporation of residual water in the zeolite. The strong indication of water loss occurring between 40°C and 100°C during the heating processes is related to the desorption of water from the surface of the grains of the powder sample. However, TGA data of hybrid PSf/Z membranes show that zeolite has an effect on membrane degradation, with the incorporation of zeolite at different compositions inducing a three-stage degradation of the membrane, compared to the

one-stage degradation observed in pure PSf.

The initial weight loss around 100 and 200°C was attributed to the desorption of water or solvent molecules previously adsorbed by the zeolite nanoparticles, which accounted for less than 5%. Stage 2, observed in the range of about 200°C to 270°C, mainly in PSf/Z 2% and 3% membranes, was attributed to the thermal rearrangement of the synthesized membrane as reported in (Samanta *et al.* 2023). The third phase, a rapid loss of material, was attributed to the decomposition of the PSf. The results showed that the (PSf/Z 0.5%) membrane started to lose weight at around 500°C slightly more than the pure PSf membrane.

On the other hand, (PSf/Z 1%, 2% and 3%) showed a decrease in the thermal stability of the membranes, as evidenced by the lower polymer decomposition temperatures compared to the (PSf/Z 0%) sample. The PSf/Z 3% membrane showed the lowest thermal stability, corresponding to the lowest decomposition temperature.

Furthermore, the residual masses remain consistently high for all membranes, depending on the zeolite content in each of the composite membranes ranging from 44% to 64%, higher than PSf/Z 0% (35.03%).

This indicates that the mass loss in these membranes is not complete, which is attributed to the presence of stable benzene rings. The decrease in thermal stability observed in the membranes produced in this study highlights the weak interfacial interaction between the PSf polymer and the zeolite particles.

3.3 Hydrophilicity, porosity and pore Size

To investigate the effect of the incorporation of zeolite nanoparticles on the hydrophilicity of PSf, the contact angle with water was measured for the (PSf/Z 0%) and (PSf/Z 3%) membranes, as shown in Fig. 3(a). The results indicate an outstanding improvement in hydrophilicity when zeolite nanoparticles are incorporated, as evidenced by the 15° decrease in contact angle from 69.6° for pure PSf to 53.3° for (PSf/Z 3%).

This increase in membrane hydrophilicity is related to the inherent hydrophilic nature of zeolite, as reported in several studies. The effect of the zeolite inclusion on the membrane porosity was investigated using the gravimetric method, and the corresponding values are shown in Fig. 3(b). The results show a significant increase in porosity with increasing zeolite content in the polymer solutions. At lower zeolite concentrations (0.5% and 1%), the membrane porosity increases to 41% and 46%, respectively, compared to the pure PSf membrane (30%). At higher zeolite concentrations (2% and 3%), the membrane porosity reaches 70% and 85% respectively, more than doubling the porosity of the pure PSf membrane.

The mean pore radius, which indicates the pore size of the different developed membranes, was also determined and shown in Fig. 3(c). The pore radius of the pure PSf membrane was around 5 nm and increased with the incorporation of the nanoparticles. The results show an increase in the pore size of the PSf/Z membranes, ranging from 5 to 22 nm, corresponding to an increase in zeolite

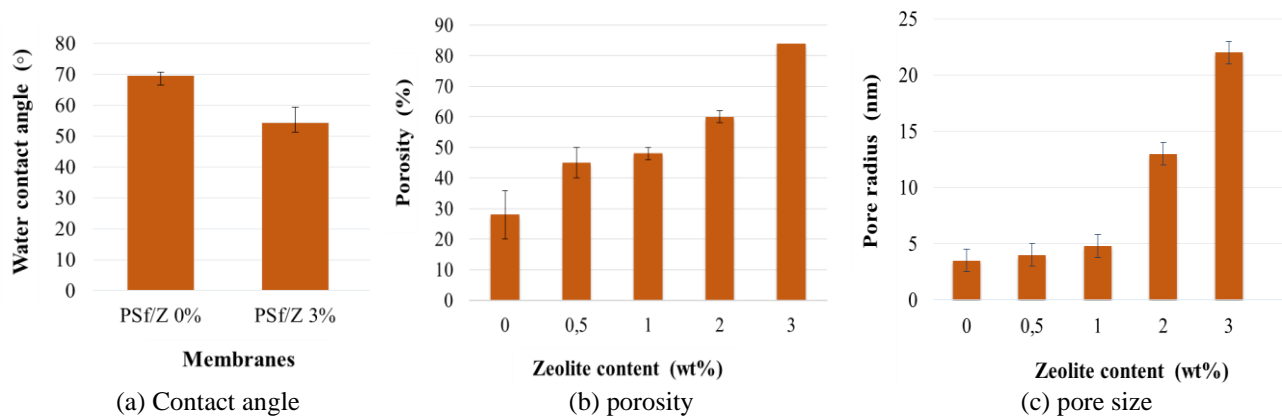


Fig. 3 Contact angle, porosity and pore size of the prepared membranes

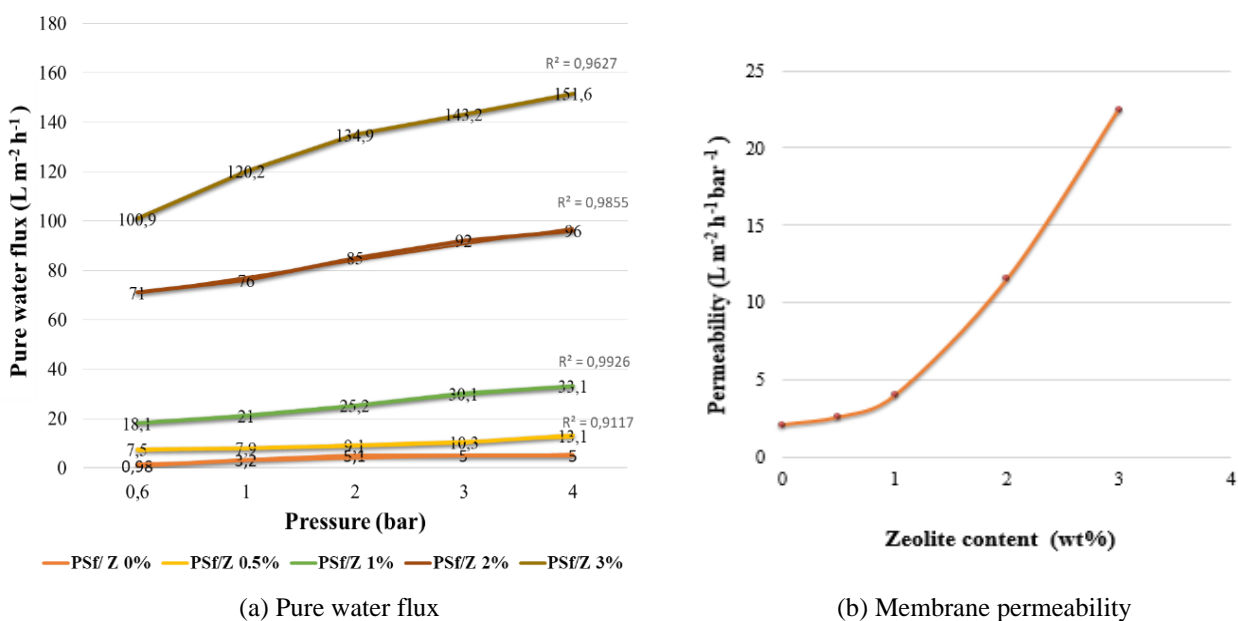


Fig. 4 Pure water flux and permeability of the prepared membranes

concentration from 0.5% to 3%. The increase in porosity and pore size could be attributed to the hydrophilic properties of the zeolite embedded in the membrane, which facilitates solvent-nonsolvent exchange during phase inversion. This process results in a more porous structure compared to the pure PSf membrane, as shown in the SEM images (Fig. 1).

3.4 Water flux and permeability

Fig. 4 shows the water flux performance of the pure PSf membrane and hybrid nanocomposite membranes with different zeolite concentrations, as a function of transmembrane pressure in the range of 0.6 - 4 bar. The process has the advantage of operating at low pressures, resulting in reduced energy consumption.

It can be seen that the pure PSf membrane (PSf/Z 0%) has a low Pure water flux of (0.89 L m⁻² h⁻¹ at 0.6 bar). However, all the hybrid membranes showed an improved PWF compared to the pure PSf membrane, with the flux increasing with the zeolite content. The 0.5% and 1% PSf/Z

membrane samples showed a slightly higher water flux than the (PSf/Z 0%) membrane.

On the other hand, the water flux shows a significant increase with the addition of 2% and 3% of zeolite nanoparticles in the membrane matrix. At 0.6 bar, the PWF increased from 7.5 to 100.9 L m⁻² h⁻¹, when the zeolite concentration was increased from 0.5 to 3 wt%. Based on the contact angle and SEM results, the observed increase in water flux was attributed to the increase in zeolite content up to a concentration of 3% zeolite in the membranes. This membrane permeation improvement can be attributed to the hydrophilic nature of zeolite, as its negatively charged aluminosilicate framework attracts water molecules through exchangeable cations and surface hydroxyl groups (Ng *et al.* 2008). Its porous structure also provides a large surface area, which further enhances its interaction with water.

The results showed that the PWF of all the hybrid membranes increased linearly with increasing transmembrane pressure. This linear correlation between the flux and transmembrane pressure strongly suggests the applicability of Darcy's law in this case (Benkhaya *et al.* 2023). The

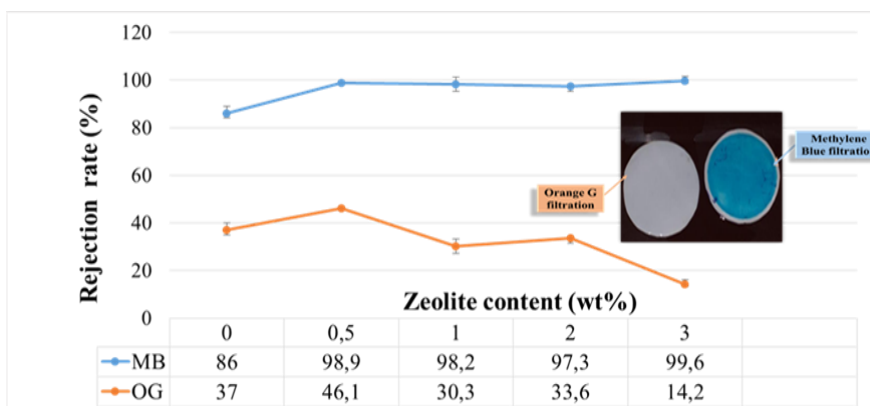


Fig. 5 MB and OG dyes removal percentage by the prepared membranes

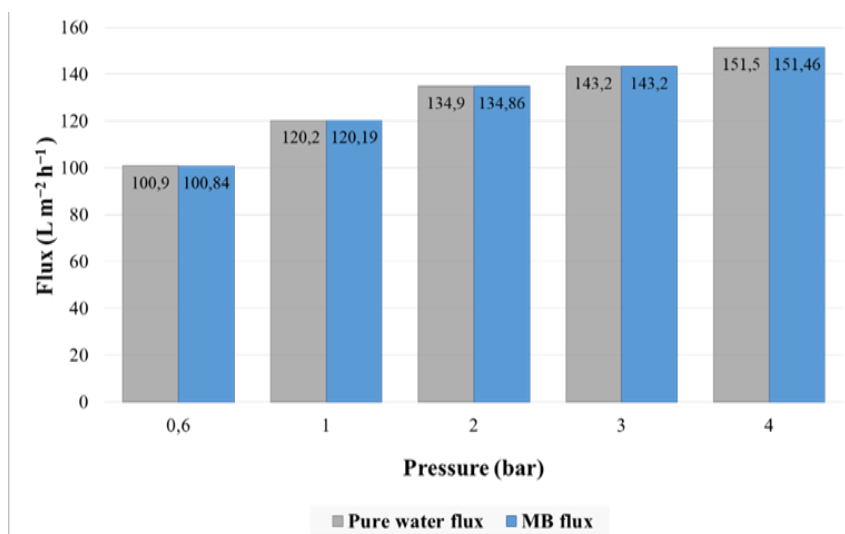


Fig. 6 Pure water and MB solution fluxes of the PSf/ Z 3% membrane

water permeability of the prepared membranes as a function of the amount of zeolite, is also shown in Fig. 4. The results show that the inherent permeability of the pure PSF membrane is relatively low, but improves with the inclusion of zeolite at different percentages. The permeability of the membrane improves from 2.2 to 22.7 L m⁻² h⁻¹ bar⁻¹, as the zeolite nanoparticle content increases from 0 to 3 wt%.

Apparently, the introduction of zeolite into the membrane matrix improves the hydraulic permeability by increasing the porosity and improving the surface hydrophilicity. In addition, the inclusion of a hydrophilic component in the membrane casting solution accelerates the exchange between solvent and non-solvent, which leads to an increase in pore size and subsequently improves the permeability of hybrid membranes (Liou *et al.* 2011).

3.5 Dyes removal

The efficiency of the composite membranes in removing methylene blue and orange G dyes is shown in Fig. 5. These selected dyes are used as templates for cationic and anionic dyes, respectively.

The removal of these dyes consisted of passing them through the different prepared membranes, and their removal

was quantified by measuring the rejection rates. To determine the concentration of the solutions before and after filtration, the absorbances of the colored solutions were measured under identical conditions. These values were then plotted on the calibration curve to determine graphically the concentration of the solution before and after filtration. The pure polysulfone membrane showed effective filtration of methylene blue dye due to its porous structure, which allows it to efficiently trap and remove the dye molecules from the solution. In addition, the adsorption rate of methylene blue by the membranes increases with the percentage of zeolite. The Methylene Blue rejection rate is particularly high, ranging from 86% to 99.6% for all the solutions used, with the PSf/Z 3% membrane showing exceptional performance in terms of Methylene Blue rejection.

This efficiency can be attributed to an electrostatic effect facilitated by the presence of zeolite. The negatively charged groups of zeolite, Si-O⁻ and Al-O⁻, on its surface play an important role in adsorption by attracting the positive charge of methylene blue (Hamid and Ismail 2020). This results in ion exchange between the support (PSf/Z) and the solute (MB). As a result, a significant amount of well-dispersed zeolite in the PSf membrane matrix contributes

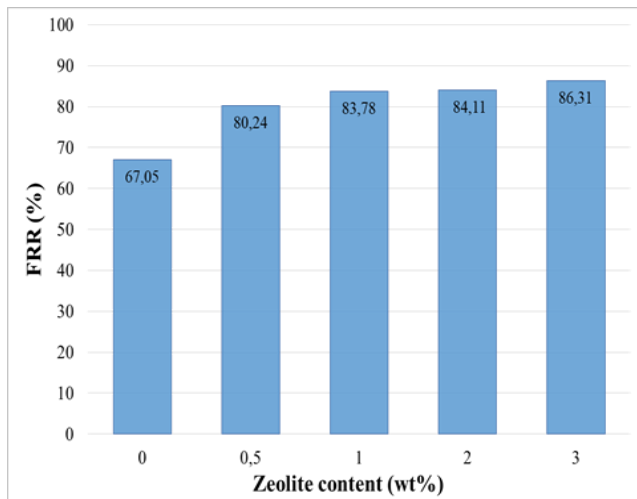


Fig. 7 Flux recovery ratio of the prepared membranes for MB solution filtration

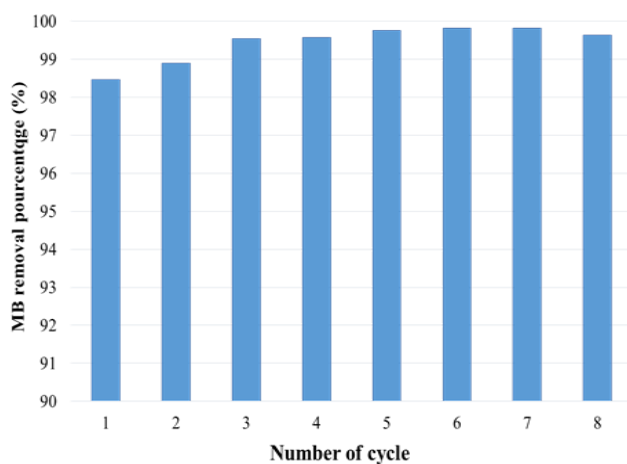


Fig. 8 Reusability test for MB filtration by PSf/Z 3% membrane

to the efficient removal of Methylene Blue from the filtered water.

As confirmed by (Brar *et al.* 2001), there is a direct correlation between the $\text{SiO}_2/\text{Al}_2\text{O}_3$ ratio and particle size distribution, where higher ratios typically produce smaller zeolite particles with increased surface areas, thereby enhancing adsorption capacity. While smaller particles optimize surface area for adsorption, larger ones, despite their lower surface area, still contribute by offering additional adsorption sites, collectively influencing the overall adsorption performance.

For Orange G rejection, the rejection rate decreases with increasing zeolite loading in the membrane matrix. The rejection rate for Orange G is relatively low, fluctuating between 46% and 14%. This divergence can be attributed to OG's smaller molecular size and planar structure, which may facilitate its passage through the membrane pores, as well as its hydrophilic nature, which limits interaction with the hydrophobic polysulfone matrix.

To evaluate the separation performance of the hybrid membrane (PSf/Z 3%), MB solution fluxes (MBF) were determined at pressures ranging from 0.6 to 4 bar, as shown

in Fig. 6. The MBF values across the membrane corresponded closely to the respective PWF values. This alignment suggests that the membrane's performance in filtering methylene blue is highly efficient and consistent with its pure water permeability. The close agreement between PWF and MBF indicates that the addition of 3% zeolite to the polysulfone matrix not only improves water flux but also maintains effective pore structure and surface properties for MB removal. This consistency demonstrates that the hydrophilicity and the porosity of the membrane, enhanced by the incorporation of zeolite, are effectively facilitate the transport of both water and methylene blue molecules across the membrane. It also suggests that the membrane's fouling resistance and adsorption capabilities are well balanced, allowing for high flux rates without significant performance degradation due to dye adsorption.

3.6 Antifouling study

After washing the membrane and re-filtering with pure water, the results (Fig. 7) show that the pure PSf membrane, had a flux recovery ratio (FRR) of 67.05%, due to its hydrophobic nature. In contrast, the incorporation of zeolite into the PSf membrane significantly increased its hydrophilicity, resulting in an improved FRR of 86.81%. The increased hydrophilicity facilitates easier removal of foulants through simple hydraulic cleaning, highlighting the membrane's excellent reversibility. Consequently, MB molecules were effectively washed off the membrane surface, resulting in good flux recovery.

This occurs because hydrophilic surfaces attract water molecules, forming a hydration layer that acts as a barrier between the membrane surface and potential foulants, thereby reducing the tendency of foulants to adhere strongly of the membrane surface (Zhang *et al.* 2016, Yang *et al.* 2019).

3.7 Reusability of the membrane

A study was carried out to evaluate the reusability of the PSf/Z 3% composite membrane used, and the findings are illustrated in Fig. 8. The membrane provided a relatively stable removal percentage of MB solution. The rejection percentage, with small decreases mainly in the first 2 hours of filtration, showed that the MB removal rate remained consistently above 98% even after undergoing eight filtration cycles.

These results confirm the efficient reusability of the PSf/Zeolite composite membranes and demonstrate their ability to maintain a high rejection rate over multiple cycles of use. The rejection rate of methylene blue (MB) using the (PSf/Z 3%) membrane increases with increasing filtration cycles, probably due to the concentration polarization layer observed had a flux recovery ratio (FRR) of 67.05%, due to its hydrophobic nature.

In contrast, the incorporation of zeolite into the PSf membrane significantly increased its hydrophilicity, resulting in an improved FRR of 86.81%. The increased hydrophilicity facilitates easier removal of foulants through simple hydraulic cleaning, highlighting the membrane's excellent reversibility.

Consequently, MB molecules were effectively washed off the membrane surface, resulting in good flux recovery.

This occurs because hydrophilic surfaces attract water molecules, forming a hydration layer that acts as a barrier between the membrane surface and potential foulants, thereby reducing the tendency of foulants to adhere strongly of the membrane surface (Zhang *et al.* 2016).

4. Conclusions

In this study, polysulfone/zeolite-Y membranes with different loading (0.5, 1, 2 and 3%) were efficiently developed using a simple phase inversion method to evaluate their efficiency in removing dyes from aqueous solution. The incorporation of hydrophilic nanofillers led to significant changes in the morphology and chemical properties of the membranes.

In addition, the presence of zeolite strongly affects the pore size, porosity, and hydrophilicity of the composite membrane. The pore size of PSf/Z gradually increased from 3 to 22 nm. The hydrophilicity of the membrane was improved by the addition of nano-Y, with a loading of 3 wt% nano-Y giving a contact angle of 54.3°. MB was successfully rejected by PSf/Z 3% ultrafiltration membranes with higher flux and rejection of about 149 L m⁻² h⁻¹ and 99.6% respectively. In contrast, the rejection rate of Orange G decreased with increasing zeolite content, can be attributed to the anionic nature and weaker binding affinity to the zeolite due to limited ion-exchange interactions. Furthermore, OG's hydrophilic properties and smaller molecular size likely reduce its interaction with the hydrophobic polysulfone matrix, resulting in lower overall removal efficiency.

Alternatively, by incorporating an optimal amount of zeolite, 3 wt%, the membrane's hydrophilicity is enhanced, thereby improving both permeate water flux (PWF) and dye rejection efficiency and resistance to fouling (FRR%) compared to neat PSf membranes. These results are promising and the approach used can be extended to other additives.

References

- Abd Hamid, S., Shahadat, M. and Ismail S. (2021), "Zeolite-polysulfone-based adsorptive membrane for removal of metal pollutants", *Chem. Pap.*, **75**(9), 4479-4492. <https://doi.org/10.1007/s11696-021-01668-x>
- Abdelhamid, A.E., El-Sayed, A.A. and Khalil, A.M. (2020), "Polysulfone nanofiltration membranes enriched with functionalized graphene oxide for dye removal from wastewater", *J. Polym. Eng.*, **40**(10), 833-841. <https://doi.org/10.1515/polyeng-2020-0141>
- Adam, M.R., Othman, M.H.D., Sheikh Abdul Kadir, S.H., Mohd Sokri, M.N., Tai, Z.S., Iwamoto, Y., ... and Jaafar, J. (2020). "Influence of the natural zeolite particle size toward the ammonia adsorption activity in ceramic hollow fiber membrane", *Membranes*, **10**(4), 63. <https://doi.org/10.3390/membranes10040063>
- Alawady, A.R., Alshahrani, A.A., Aouak, T.A. and Alandis N.M. (2020), "Polysulfone membranes with CNTs/Chitosan biopolymer nanocomposite as selective layer for remarkable heavy metal ions rejection capacity", *Chem. Eng. J.*, **388**, 124267. <https://doi.org/10.1016/j.cej.2020.124267>
- Ali, A.S.M., Soliman, M.M., Kandil, S.H. and Khalil, M.M. (2021), "Emerging mixed matrix membranes based on zeolite nanoparticles and cellulose acetate for water desalination", *Cellulose*, **28**(10), 6417-6426. <https://doi.org/10.1007/s10570-021-03924-5>
- Asif, K., Lock, S.S.M., Taqvi, S.A.A., Jusoh, N., Yiin, C.L., Chin, B.L.F. and Loy, A.C.M. (2021), "A molecular simulation study of silica/polysulfone mixed matrix membrane for mixed gas separation", *Polymers*, **13**(13), 2199. <https://doi.org/10.3390/polym13132199>
- Badrinezhad, L., Ghasemi, S., Azizian-Kalandaragh Y. and Nematollahzadeh, A. (2018), "Preparation and characterization of polysulfone/graphene oxide nanocomposite membranes for the separation of methylene blue from water", *Polym. Bull.*, **75**, 469-484. <https://doi.org/10.1007/s00289-017-2046-7>
- Banerjee, S., Dubey, S., Gautam, R.K., Chattopadhyaya, M.C. and Sharma, Y. (2019), "Adsorption characteristics of alumina nanoparticles for the removal of hazardous dye, Orange G from aqueous solutions", *Arab. J. Chem.*, **12**(8), 5339-5354. <https://doi.org/10.1016/j.arabjc.2016.12.016>
- Benkhaya, S., Lgaz, H., Alrashdi, A.A., M'rabet, S., El Bachiri, A., Assouag, M., Chung, I.M. and El Harfi, A. (2021), "Upgrading the performances of polysulfone/polyetherimide ultrafiltration composite membranes for dyes removal: Experimental and molecular dynamics studies", *J. Mol. Liq.*, **331**, 115743. <https://doi.org/10.1016/j.molliq.2021.115743>
- Benkhaya, S., Lgaz, H., Tang, H., Altaee, A., Haida, S., Vatanpour, V. and Xiao, Y. (2023), "Investigating the effects of polypropylene/TiO₂ loading on the performance of polysulfone/polyetherimide ultrafiltration membranes for azo dye removal: Experimental and molecular dynamics simulation", *J. Water Process Eng.*, **56**, 104317. <https://doi.org/10.1016/j.jwpe.2023.104317>
- Brar, T., France, P. and Smirniotis, P.G. (2001), "Control of crystal size and distribution of zeolite A". *Ind. Eng. Chem. Res.*, **40**(4), 1133-1139. <https://doi.org/10.1021/ie000748q>
- Cheikh S'Id, E., Kheribech, A., Degu, M., Hatim, Z., Chourak, R. and M'Bareck, C., (2021), "Removal of methylene blue from water by polyacrylonitrile Co sodium methallylsulfonate copolymer (AN69) and polysulfone (PSf) synthetic membranes", *Prog. Color Colorants Coat.*, **14** (2), 89-100. <https://doi.org/10.30509/pccc.2021.81690>
- Dorosti, F., Omidkhah, M., Pedram, M. and Moghadam, F. (2011), "Fabrication and characterization of polysulfone/ polyimide-zeolite mixed matrix membrane for gas separation", *Chem. Eng. J.*, **171**(3), 1469-1476. <https://doi.org/10.1016/j.cej.2011.05.081>
- Ghribi, F., Boudjema, A., Benmaamar, Z. and Bachari, K. (2022), "Preparation and enhanced visible-light photo-catalytic dye degradation activity of NiZY composites", *Biointerf. Res. Appl. Chem.*, **13**, 1-12. <https://doi.org/10.33263/BRIAC131.072>
- Hamid, S. and Ismail S. (2020), "Effect of Sodium Dodecyl Sulfate (SDS) on Polysulfone/Zeolite membrane for the removal of copper ions", *IOP Conference Series: Materials Science and Engineering*, *IOP Publishing*, **796**(1), 012053. <https://doi.org/10.1088/1757-899X/796/1/012053>
- He, Y., Li, J., Liu, C., Zhao, L., Wang, Z., Yang, J., Zhou, L. and Gou, S. (2023), "Synergistic effect between montmorillonite and imidazolium-functionalized carboxylate-based polyelectrolyte for enhancing the removal of methylene blue", *J. Water Process Eng.*, **56**, 104518. <https://doi.org/10.1016/j.jwpe.2023.104518>
- Hung, W.L., Wang, D.M., Lai, J.Y. and Chou, S.C. (2016), "On the initiation of macrovoids in polymeric membranes—effect of polymer chain entanglement", *J. Membr. Sci.*, **505**, 70-81.

- <https://doi.org/10.1016/j.memsci.2016.01.021>
- Ibrahim, G.S., Isloor, A.M., Al Ahmed, A. and Lakshmi, B., (2016), "Fabrication and characterization of polysulfone-zeolite ZSM-5 mixed matrix membrane for heavy metal ion removal application", *J. Appl. Membr. Sci. Technol.*, **18**(1).
<https://doi.org/10.11113/amst.v18i1.17>
- Imam, S., Muhammad, A. I., Babamale, H.F. and Zango, Z.U. (2021), "Removal of orange G dye from aqueous solution by adsorption: a short review", *J. Environ. Treat. Tech.*, **9**(1), 318-327. [https://doi.org/10.47277/JETT/9\(1\)327](https://doi.org/10.47277/JETT/9(1)327)
- Laksaci, H., Khelifi, A., Belhamdi, B. and Trari, M. (2019), "The use of prepared activated carbon as adsorbent for the removal of orange G from aqueous solution", *Microchem. J.*, **145**, 908-913. <https://doi.org/10.1016/j.microc.2018.12.001>
- Lekena, N., Makhetha, T.A. and Moutloali, R.M. (2023), "Polyacrylonitrile ultrafiltration membranes incorporating graphene oxide fillers modified with Zeolitic Imidazolate Framework-8 and 3-aminopropyltriethoxysilane for dye and salt removal in real textile wastewater", *J. Environ. Chem. Eng.*, **11**(5), 110883. <https://doi.org/10.1016/j.jece.2023.110883>
- Liou, R.M., Chen, S.H., Lai, C.L., Hung, M.Y. and Huang, C.H. (2011), "Effect of ammonium groups of sulfonated polysulfone membrane on its pervaporation performance", *Desalination*, **278**(1-3), 91-97. <https://doi.org/10.1016/j.desal.2011.05.006>
- Liu, F., Ma, B.R., Zhou, D., Xiang, Y.H., Xue, L.X. (2014), "Breaking through tradeoff of Polysulfone ultrafiltration membranes by zeolite 4A", *Micropor. Mesopor. Mater.*, **186**, 113-120. <https://doi.org/10.1016/j.micromeso.2013.11.044>
- Mokhtari, S., Rahimpour, A., Shamsabadi, A.A., Habibzadeh, S. and Soroush, M. (2017), "Enhancing performance and surface antifouling properties of polysulfone ultrafiltration membranes with salicylate-alumoxane nanoparticles", *Appl. Surf. Sci.*, **393**, 93-102. <https://doi.org/10.1016/j.apsusc.2016.10.005>
- Moradihamedani, P. (2022), "Recent advances in dye removal from wastewater by membrane technology: A review", *Polym. Bull.*, **79**(4), 2603-2631.
<https://doi.org/10.1007/s00289-021-03603-2>
- Nadour, M., Boukraa, F., Ouradi, A. and Benaboura A. (2017), "Effects of methylcellulose on the properties and morphology of polysulfone membranes prepared by phase inversion", *Mater. Res.*, **20**(2), 339-348.
<https://doi.org/10.1590/1980-5373-MR-2016-0544>
- Ng, E.P. and Mintova, S. (2008), "Nanoporous materials with enhanced hydrophilicity and high water sorption capacity", *Micropor. Mesopor. Mater.*, **114**(1-3), 1-26.
<https://doi.org/10.1016/j.micromeso.2007.12.022>
- Ouradi, A., Cherifi, N., Nguyen, Q. T. and Benaboura, A. (2020), "Preliminary study of the prepared polysulfone/AN69/clay composite membranes intended for the hemodialysis application", *Chem. Pap.*, **74**, 2133-2144.
<https://doi.org/10.1007/s11696-020-01062-z>
- Rana, J., Goindi, G., Kaur, N., Krishna, S. and Kakati, A. (2022), "Synthesis and application of cellulose acetate-acrylic acid/acrylamide composite for removal of toxic methylene blue dye from aqueous solution", *J. Water Process Eng.*, **49**, 103102.
<https://doi.org/10.1016/j.jwpe.2022.103102>
- Routoula, E. and Patwardhan, S.V. (2020), "Degradation of anthraquinone dyes from effluents: a review focusing on enzymatic dye degradation with industrial potential", *Environ. Sci. Technol.*, **54**(2), 647-664.
<https://doi.org/10.1021/acs.est.9b03737>
- Salam, M.A., Kosa, S.A. and Al-Beladi, A.A. (2017), "Application of nanoclay for the adsorptive removal of Orange G dye from aqueous solution", *J. Mol. Liq.*, **241**, 469-477.
<https://doi.org/10.1016/j.molliq.2017.06.055>
- Samanta, N.S., Mondal, P., Dhara, S., Bora, U. and Purkait, M.K. (2023), "Fabrication of LD-slag derived zeolite Y coated polysulfone (PSf) membrane for decontamination of groundwater", *Chem. Eng. J.*, **478**, 147330.
<https://doi.org/10.1016/j.cej.2023.147330>
- Sharma, N. and Purkait, M.K. (2017), "Fabrication and characterization of polysulfone ultrafiltration membrane using polyethylene glycol and tartaric acid: morphology and performance in protein separation", *Membr. Water Treat.*, **8**(6), 591-612. <https://doi.org/10.12989/mwt.2017.8.6.591>
- Shi, W., Gao, F., Li, X. and Wangm Z. (2022), "High zeolite loading mixed matrix membrane for effective removal of ammonia from surface water", *Water Res.*, **221**, 118849.
<https://doi.org/10.1016/j.watres.2022.118849>
- Vakili, M., Gholami, F., Zwain, H. M., Wang, W., Mojiri, A., Gholami, Z., Tomas, M., Giwa, A. S. and Cagnetta, G. (2023), "Treatment of As (III)-contaminated food waste using alkali treatment and its potential application for methylene blue removal from aqueous solutions", *J. Water Process Eng.*, **55**, 104100. <https://doi.org/10.1016/j.jwpe.2023.104100>
- Vedula, S.S. and Yadav, G.D. (2022), "Wastewater treatment containing methylene blue dye as pollutant using adsorption by chitosan lignin membrane: Development of membrane, characterization and kinetics of adsorption", *J. Indian Chem. Soc.*, **99**(1), 100263. <https://doi.org/10.1016/j.jics.2021.100263>
- Yang, X., Liu, L. and Jiang, S. (2019), "Enhancement of hydrophilicity and anti-fouling property of polysulfone membrane using amphiphilic nanocellulose as hydrophilic modifier", *Membr. Water Treat.*, **10**(6), 461-469.
<https://doi.org/10.12989/mwt.2019.10.6.461>
- Zhang, R., Liu, Y., He, M., Su, Y., Zhao, X., Elimelech, M. and Jiang, Z. (2016), "Antifouling membranes for sustainable water purification: Strategies and mechanisms", *Chem. Soc. Rev.*, **45**(21), 5888-5924. <https://doi.org/10.1039/C5CS00579E>
- Zhu, S., Zhang, X., Dong, L., Yuan, Y., Ma, X., Chen, Y. and Xu, L. (2024), "Synthesis of a hierarchical TS-1 zeolite with tunable macropore size and its performance in the catalytic oxidation reactions", *CrystEngComm*, **26**(38), 5469-5478.
<https://doi.org/10.1039/D4CE00706A>

CC